



OPEN ACCESS

EDITED BY
Michael Fleming,
Organisation For Economic Co-Operation
and Development, France

REVIEWED BY
Jiankai Yu,
Massachusetts Institute of Technology,
United States
Oliver Buss,
Organisation For Economic Co-Operation
and Development, France
Thomas M. Miller,
Oak Ridge National Laboratory (DOE),
United States

*CORRESPONDENCE
Yosuke Iwamoto,
✉ iwamoto.yosuke@jaea.go.jp

SPECIALTY SECTION
This article was submitted
to Nuclear Energy,
a section of the journal
Frontiers in Energy Research

RECEIVED 31 October 2022
ACCEPTED 16 January 2023
PUBLISHED 25 January 2023

CITATION
Iwamoto Y, Tsuda S and Ogawa T (2023),
Benchmark shielding calculations for
fusion and accelerator-driven sub-
critical systems.
Front. Energy Res. 11:1085264.
doi: 10.3389/fenrg.2023.1085264

COPYRIGHT
© 2023 Iwamoto, Tsuda and Ogawa. This
is an open-access article distributed under
the terms of the [Creative Commons
Attribution License \(CC BY\)](https://creativecommons.org/licenses/by/4.0/). The use,
distribution or reproduction in other
forums is permitted, provided the original
author(s) and the copyright owner(s) are
credited and that the original publication in
this journal is cited, in accordance with
accepted academic practice. No use,
distribution or reproduction is permitted
which does not comply with these terms.

Benchmark shielding calculations for fusion and accelerator-driven sub-critical systems

Yosuke Iwamoto*, Shuichi Tsuda and Tatsuhiko Ogawa

Nuclear Science and Engineering Center, Japan Atomic Energy Agency, Ibaraki, Japan

We conducted benchmark calculations of neutron-shielding experiments for fusion applications such as (1) Neutron spectra in iron shields with 14 MeV neutrons; and (2) Leakage neutron spectra from various sphere piles by 14 MeV neutrons, and for Accelerator-Driven Sub-Critical system (ADS) such as (3) Neutron energy spectra after transmission through iron and concrete shields using a quasi-monochromatic neutron source, (4) Thick target neutron yield produced by high-energy heavy ion incidence on a thick target, and (5) Induced radio activity in concrete exposed to secondary particles produced by heavy-ion incident reaction on an iron target by using the Particle and Heavy Ion Transport code System (PHITS). For case (1), the calculated neutron energy spectra using the nuclear data libraries, JENDL-4.0, agreed with the experimental data in iron shields. For the cases (2) of Al, Ti, Cr, and As piles, the neutron energy spectra calculated with JENDL-4.0 agreed with the experimental results well. For the case (3), the neutron spectra calculated with JENDL-4.0/HE reproduced the experimental data because the proton data library of ${}^7\text{Li}$ can produce source neutrons for proton incident reactions. For the case (4), calculated results for thick target neutron spectra produced by a 400 MeV per nucleon carbon incident reaction on lead reproduced the experimental data well. For the case (5) with a neutron source produced by the 200–400 MeV per nucleon heavy-ion incident reaction, the calculated results of the reaction rate depth profiles of ${}^{197}\text{Au}(n, \gamma){}^{198}\text{Au}$ reactions reproduced the experimental results within a factor of 2. Overall, PHITS with nuclear data libraries reproduced the experimental data sufficiently well. Thus, PHITS has a potential application in the design of advanced reactor systems, such as fusion and ADS facilities. This experimental data are also useful in validating nuclear reaction models in other Monte Carlo codes and evaluating nuclear data libraries for advanced reactor systems.

KEYWORDS

neutron, shielding, benchmark, fusion, ADS, PHITS

1 Introduction

A fusion nuclear facility is one of the most advanced reactor systems in the high-energy region. Nuclear fusion is a process to fuse two lighter nuclei to form one heavier nucleus, which releases a large amount of energy. Fusion reactions occur in a matter at a state called plasma, which is a hot mixture composed of positive ions and freely moving electrons. Plasma has unique properties different from those of solids, liquids, and gases. The reaction between two hydrogen isotopes, deuterium (D) and tritium (T), is the most efficient fusion reaction. The International Thermonuclear Experimental Reactor (ITER) is an international research project aimed at producing energy through fusion processes. It is the first fusion device to produce energy continuously by chain reactions; ITER will test the integrated technologies, materials, and physical regimes necessary to commercially produce electricity from fusion.

Fusion neutron engineering is one of the most important issues in the development of fusion reactors, which studies various nuclear parameters. D-T neutrons interact with steel materials as structural materials for blankets and diverters, SiC/SiC composites as functional materials, copper alloys as heat sink and cooling tube materials, and tungsten as counterpart materials for high load parts, causing nuclear heating and induced radioactivity production, along with tritium breeding. In particular, the tritium breeding ratio is the most important parameter in terms of fuel self-sufficiency. Fusion reactor design involves concerns such as radiation shielding, material heating, and displacement damage. Activation is also an important concern in terms of dose rate, heat generation, and radioactive waste management. These evaluations are essential to obtain approval for equipment construction in terms of radiation safety. Important parameters in activation are products of the interaction between neutrons and materials. On the other hand, the effects of gamma irradiation must be considered in radiation shielding design and material aging. Tritium treatment is also important from the viewpoint of radiation protection. The nuclear design of a fusion reactor relies on currently-available computational codes and data. These include Monte Carlo particle codes and related data libraries such as neutron cross sections and neutron activation cross sections. In order to accurately evaluate the above nuclear parameters, the codes and data applied to the design calculations need to be validated using experimental data. Fusion neutron engineering research began in Japan in the early 1980s. The high-intensity D-T neutron facilities, i.e., the Fusion Neutronics Source (FNS) at the Japan Atomic Energy Research Institute (JAERI, now the Japan Atomic Energy Agency) and the OKTAVIAN at Osaka University, are the world's leading facilities providing experimental data related to fusion research (Konno et al., 1991; Sub Working Group of Fusion Reactor Physics Subcommittee, 1994). Fundamental integral benchmark experiments were performed in these facilities for fusion applications. These integral experiments were performed using the D-T neutron source, with simple geometry and materials.

The Accelerator-Driven Sub-Critical system (ADS) is also one of the advanced reactor systems. In this system, the transmutation and separation of actinides and some long-lived fission products from nuclear production produced in a fission reactor can reduce the radio-toxicity of high-level waste to one-hundredth that of the current once-through fuel cycle (Mukaiyama et al., 2001). Only fission reactors and spallation sources are available in the medium term because of the high intensity required for transmutation. The concept of ADS combines a proton particle accelerator using an energy of around 1 GeV with a sub-critical core. Protons are incident on a spallation target made up of solid or liquid heavy metals, such as a lead bismuth eutectic alloy, that produces source neutrons to drive a subcritical reactor. The spallation reaction at the target produces dozens of neutrons per incident proton and introduces them into the subcritical core. It is similar to a critical reactor core, except that it is subcritical. In the design of an ADS facility, the behavior of spallation neutrons in the material and radiation shielding must be studied as well as those in fusion devices as described above. It should be noted that the maximum neutron energy is 14 MeV for fusion. The maximum neutron energy for ADS is around the energy of the maximum energy of the proton for a proton driven system. Therefore, experimental data on high-energy neutron shielding is required to validate nuclear reaction models in the Monte Carlo (MC) code and data libraries used for fusion and ADS design calculations. The nuclear reaction model of the intranuclear cascade

model + evaporation model is used for energies above the table based cross sections. Shielding experiments for neutrons have been performed at the Takasaki Ion Accelerator for Advanced Radiation Application (TIARA) (Nakao et al., 1996; Nakashima et al., 1996) and the Heavy Ion Medical Accelerator in Chiba (HIMAC) at the National Institute of Radiological Science (NIRS) (Kurosawa et al., 1999; Satoh et al., 2007; Ogawa et al., 2011). These facilities have achieved results in fundamental benchmark experiments for accelerator applications. These neutron shielding experiments have been performed using a neutron source with a 40–70 MeV proton-lithium nuclear reaction, a neutron source with a 230–400 MeV/u helium, and various ions with 100–800 MeV/u incident nuclear reaction on a thick target.

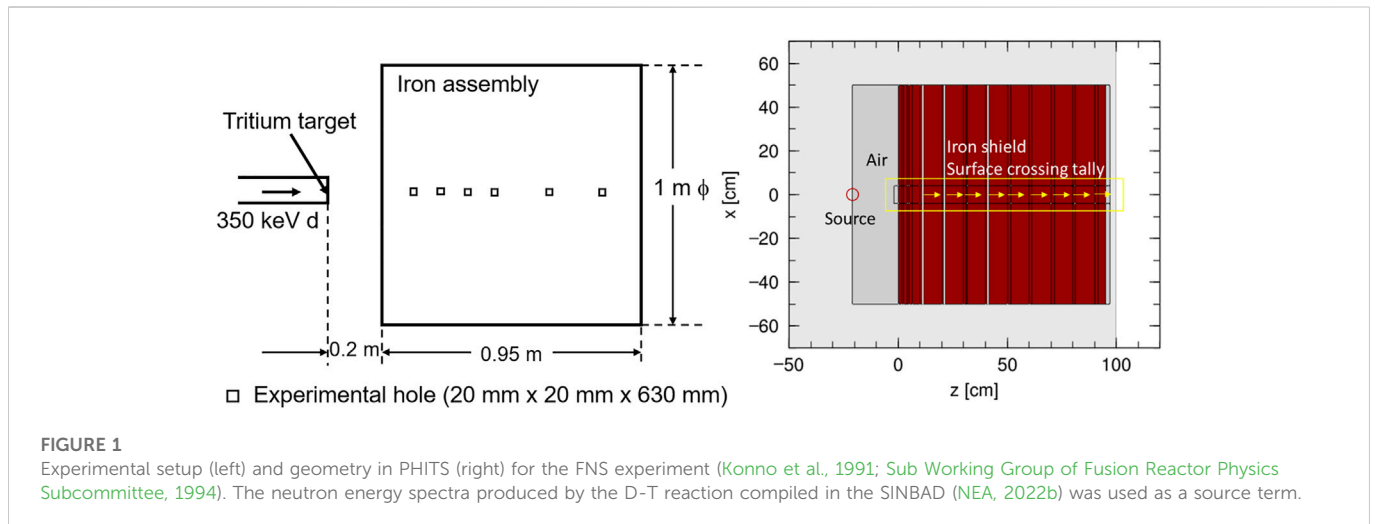
The experimental data needs to be reviewed and then compared to the results calculated with nuclear reaction models and nuclear data libraries so as to validate nuclear reaction models and nuclear data in the design of advanced reactor systems in the high-energy region. Therefore, it is desirable for benchmark calculations to use the shielding integral benchmark archive and database (SINBAD) [9–11].

In this paper, our developing MC code, the Particle and Heavy Ion Transport code (PHITS) (Iwamoto et al., 2017; Sato et al., 2018), was validated with the experimental data included in the SINBAD database and our experimental data. This paper is organized as follows. Section 2 presents experimental and calculation conditions of two experiments related with fusion and three experiments related with accelerator-shielding, which were generated from (1) Integral experiment on iron cylindrical assembly with D-T neutron source at FNS (Konno et al., 1991; Sub Working Group of Fusion Reactor Physics Subcommittee, 1994), (2) Leakage neutron spectra from various sphere piles with D-T neutron source at OKTAVIAN, Osaka university (Sub Working Group of Fusion Reactor Physics Subcommittee, 1994), (3) Neutron energy spectra after transmission through shields using a quasi-monochromatic neutron source at TIARA (Nakao et al., 1996; Nakashima et al., 1996), (4) Thick target neutron yield produced by high-energy heavy-ion incident reaction at HIMAC (Kurosawa et al., 1999; Satoh et al., 2007), and (5) Induced activity in shield exposed to particles produced by heavy-ion on Fe at HIMAC (Ogawa et al., 2011). For the cases of (3), (4), and (5), the benchmark studies have been conducted in our previous paper and report (Ogawa et al., 2011; NEA, 2022b; Iwamoto et al., 2022). In this paper, we introduce a part of our benchmark study for these cases and present a new benchmark calculation with PHITS for the case of (1) and (2). Section 3 presents the benchmark results and discussion in all cases, and Section 4 shows the summary of this research work.

2 Experiments and calculation procedure

2.1 Overview of the PHITS code

PHITS (Iwamoto et al., 2017; Sato et al., 2018) is a general-purpose Monte Carlo particle transport code. It can deal with the transport of all particles over wide energy ranges, using several nuclear reaction models and nuclear data libraries. For the PHITS nuclear reaction models, the Liège intranuclear cascade model (INCL4.6) (Boudard et al., 2013) is used for neutrons above 20 MeV and protons above 1 MeV. The JAERI Quantum Molecular Dynamics (JQMD) model (Ogawa et al., 2015) is used for nucleus above 10 MeV/u. These models are coupled with the evaporation model GEM (Furihata, 2000), which handles the statistical decay of the spallation residues. The nuclear data



library, JENDL-4.0 (Shibata et al., 2011), is used for neutrons below 20 MeV. For the case (3), the high-energy nuclear data library, JENDL-4.0/HE (Kunieda et al., 2016), is also used for protons and neutrons below 200 MeV.

The weight window variance reduction method in PHITS is similar to that in the MCNP code (Goorley et al., 2012). Particle weights are affected by importance, forced collisions, implicit capture, and the weight window function. If the weight is lower than a user-defined weight cutoff, a Russian roulette method is applied to determine if the particle should be killed. In PHITS, the weight window defined in the weight widow section is automatically determined by the weight window generator section.

2.2 Experimental conditions

This subsection describes the experimental condition of five experiments.

2.2.1 Integral experiment on iron cylindrical assembly at FNS

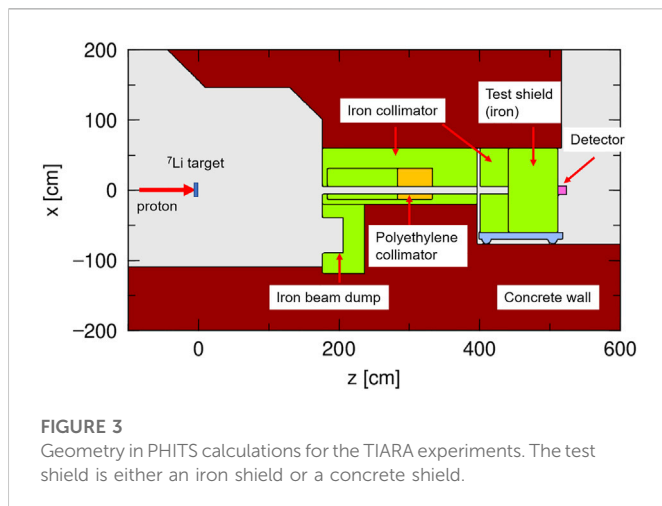
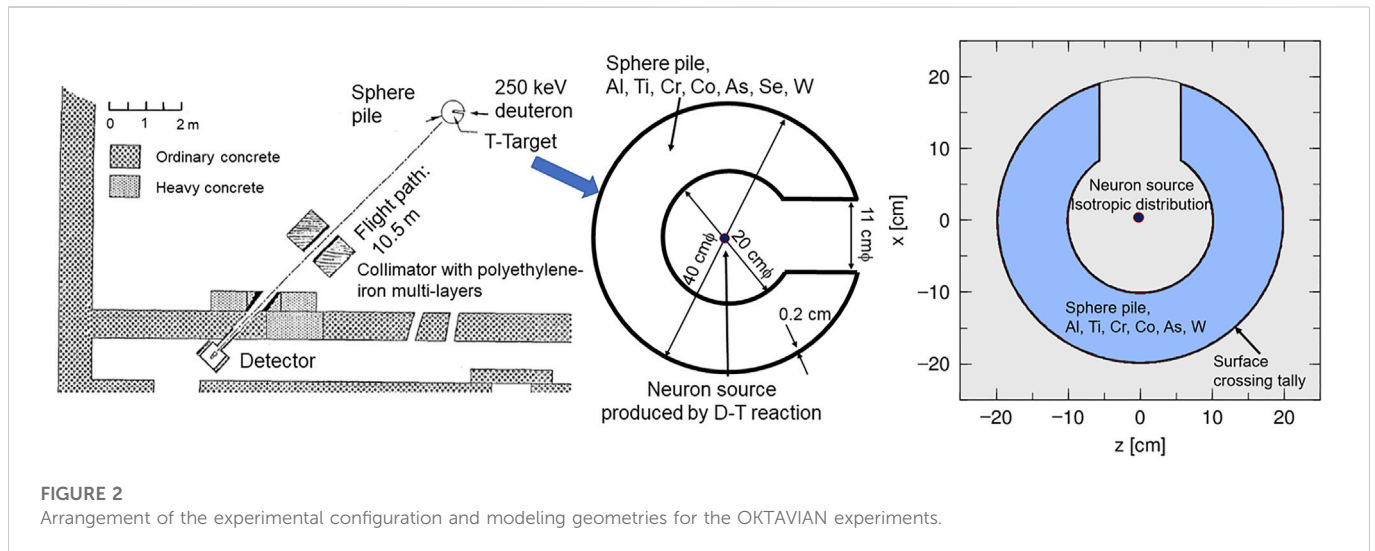
Figure 1 shows the experimental setup with a 0.95-m-thick-iron and calculation geometry for the FNS experiment. The experimental data and the calculation geometry of the integral experiment on the iron cylindrical assembly at the FNS were compiled in the SINBAD abstract NEA-1553/45 (Kodeli et al., 2006; NEA, 2022a; ORNL, 2022). The experiment was done in the first target room of the FNS facility of JAERI (Konno et al., 1991; Sub Working Group of Fusion Reactor Physics Subcommittee, 1994). Neutrons were produced by D-T nuclear reaction. A 350 keV deuteron beam with 0.5–150 μ A current was incident on a water-cooled Tritium-Titanium (T-T) target. The activity of tritium was 3.7×10^{11} Bq. Neutron at the tritium target were measured by the alpha particle counting method with an accuracy of about 3%. The iron shield with 1 m diameter and 0.95 m thickness was placed 0.2 m from the T-T target. Impurities include 0.148 wt% S, 0.834 wt% Mn, and 0.185 wt% C. It has 6 holes (20 \times 20 \times 630 mm) in the radial direction. The proton recoil gas counter was placed into the 6 holes inside the iron assembly to measure neutron spectra with energies from a few keV to 1 MeV. The center locations of the holes were 0.11, 0.21, 0.31, 0.41, 0.61, and

0.81 m from the front of the iron shield. The number of incident neutrons was monitored at the front of the iron shield. Total neutron yields ranged from 9.4×10^{11} – 2.8×10^{14} . The calculation geometry in PHITS was taken from the MCNP input in the SINBAD abstract NEA-1553/45. The neutron energy spectra of the D-T source compiled in the SINBAD abstract were employed as a source term in the PHITS calculation. Neutrons were emitted in isotropic direction. The nuclear data library, JENDL-4.0 (Shibata et al., 2011), was used for the transport calculation of neutrons in the iron assembly. Neutron energy spectra in the iron assembly were tallied at each depth with the [t-cross] tally, which is the surface crossing tally for neutrons. The flux tally is representative for the flux on the surface with 4 cm radius of the block.

2.2.2 Leakage neutron spectra from various sphere piles with D-T neutrons

The experimental data and the calculation geometry of the leakage neutron spectra from various sphere piles with D-T neutrons at OKTAVIAN were compiled in the SINBAD abstract NEA-1553/45 (Kodeli et al., 2006; NEA, 2022a; ORNL, 2022). The experiment was conducted at the beam line of OKTAVIAN (Sub Working Group of Fusion Reactor Physics Subcommittee, 1994). A 250 keV deuteron beam was incident on a 370 GBq tritium target to produce neutrons. Figure 2 shows the experimental set-up and calculation geometry. The 40-cm diameter sphere piles were used for the piles of aluminum, titanium, chromium, cobalt, arsenic, and tungsten. There is a layer of 0.2-cm thick stainless steel (JIS SUS-304) around the 40-cm diameter sphere pile. The pile has a 20 cm diameter void and an 11 cm diameter re-entrant hole through which the target beam duct can pass. A target was set at the center of the pile. This pile was replaced after each measurement. The neutron source spectra given in (Sub Working Group of Fusion Reactor Physics Subcommittee, 1994) were obtained with the time-of-flight (TOF) technique. Note that the references 1 and the SINBAD abstract NEA-1553/45 contain no information about the tritium target. The neutron energy spectrum listed in reference 1 was used as a source term and neutrons were emitted isotropically in the calculation.

The liquid organic scintillator NE-218 to measure neutrons was positioned at 55° to the beam direction and 10.5 m from the target.



Detailed information on the collimator system is available in reference 1. A collimator with multi-layer polyethylene and iron was placed between the detector and the sphere pile to decrease the background events. The absolute value of the leakage neutron yield from the pile is obtained by the gamma-rays intensity of the induced radioactivity of ^{92m}Nb , a niobium foil in front of the target, and the number of the integrated source neutron spectrum (Sub Working Group of Fusion Reactor Physics Subcommittee, 1994).

The simplified calculation geometry in PHITS was taken from the MCNP input in the SINBAD abstract NEA-1553/45 (Kodeli et al., 2006; NEA, 2022a; ORNL, 2022). The neutron transport was calculated by using JENDL-4.0. The neutrons that penetrated through a pile were scored with the [t-cross] tally, and the neutron energy spectra of source compiled in the SINBAD were used as a source term in the PHITS calculation.

2.2.3 Transmuted neutron energy spectra through shields using a quasi-monoenergetic neutrons

The shielding experiments were performed for iron and concrete shields with quasi-monoenergetic neutron sources with energies of 41- and 65-MeV developed at TIARA. Quasi-monoenergetic neutrons were produced by the 43- and 68-MeV proton incident reaction on

lithium. In this experiment, neutron energy spectra transmitted through 25- to 200-cm-thick concrete shields (Nakao et al., 1996) and through 10- to 130-cm-thick irons (Nakashima et al., 1996) were obtained by using Bonner ball sphere detectors and a liquid scintillator BC501A. The neutron spectrum in the energy region between a few MeV and a peak energy were obtained with a BC501A and thermal neutrons with energies below a few MeV were obtained from Bonner ball measurements.

Figure 3 shows the calculation geometry with PHITS for TIARA experiments (Kos and Kodeli, 2019).

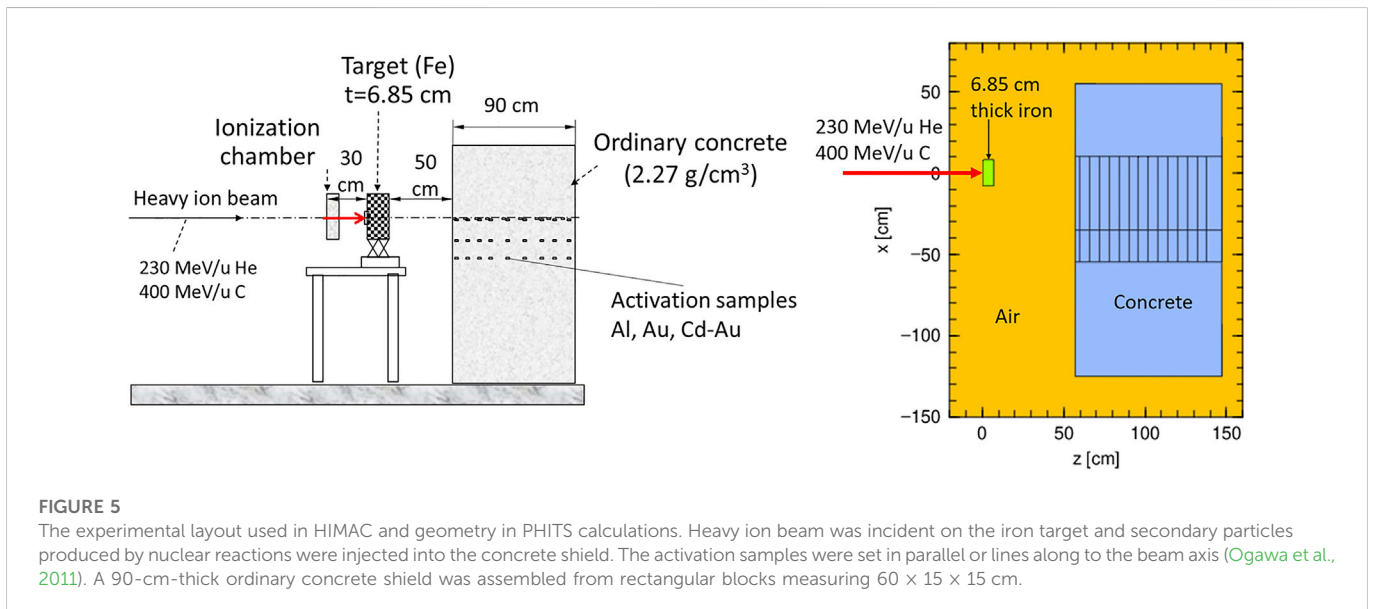
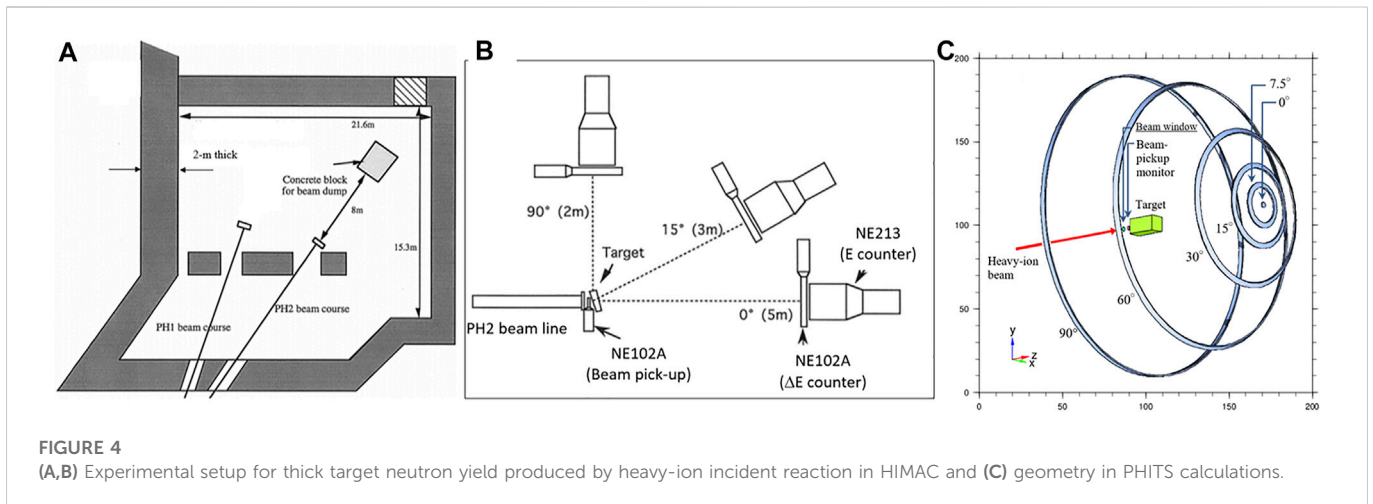
The targets were 3.6-mm and 5.2-mm thick lithium (99.9% enriched ^7Li) for the 43- and 68-MeV proton, respectively. Neutrons went through an iron collimator with 10.9-cm-diameter and experimental assembly. The protons that penetrated the target were bent downward to the iron beam dump by the magnetic field. The 25–200 cm thick concrete shields were assembled with $120 \times 120 \times 25$ cm thick plates and the 10–130 cm thick steel shields were assembled with $120 \times 120 \times 10$ cm thick plates. The concrete density was 2.31 g/cm^3 and the iron density was 7.87 g/cm^3 .

The contribution of the neutrons generated by the iron beam dump to the detector is negligible. The proton incident reaction on lithium was simulated with the physics model, INCL4.6 (Boudard et al., 2013), or the proton data library for JENDL-4.0/HE (Kunieda et al., 2016).

2.2.4 Thick target neutron yield produced by heavy-ion incident reaction

Secondary neutron yields from thick targets (Kurosawa et al., 1999; Satoh et al., 2007) of graphite, aluminum, copper, and lead irradiated with heavy-ions from helium to xenon with energies of 100–800 MeV/u were obtained at HIMAC of NIRS, compiled in the SINBAD abstract NEA-1552/35 (Kodeli et al., 2006; NEA, 2022a; ORNL, 2022). The neutron yields from materials produced by heavy-ion-induced reactions were used as the source term for the neutron shielding experiment at HIMAC (Kurosawa et al., 1999). The thicknesses of the materials varied depending on the ion energy so as to ensure that the ions come to a complete stop within the target.

The experiment was performed in the general-purpose irradiation room (PH2) beam line shown in Figure 4A. Room



walls, made of 2-m-thick concrete, were located at least 8 m away from the target in all directions, except for the pillars near the target. The concrete ceiling was located about 6 m above the target, and the floor was about 1.25 m below the target. The distance from the target to the beam dump surface was set to be 8.0 m.

Figure 4B shows a schematic view of the typical arrangement of target and detectors. Neutron energy produced in the target was obtained by TOF between the beam pick-up detector set in front of the target and a liquid organic scintillator (NE213, 12.7 cm in diameter, 12.7 cm long), located at 0° , 7.5° , 15° , 30° , 60° , and 90° . Figure 4C shows geometry in PHITS calculations for the experiment of thick target neutron yields.

Regarding the radiation transport calculation, the INCL4.6 model was employed for nucleons and light particles (proton, deuteron, triton, and alpha) and the JQMD model (Ogawa et al., 2015) was used for nucleus. JENDL-4.0 was applied for neutrons below 20 MeV.

2.2.5 Induced radioactivity in shield exposed to secondary particles produced by heavy ions on Fe

The experiments were performed at the PH1 of HIMAC at NIRS (Ogawa et al., 2011) where heavy ion beams of several 100 MeV/u are available. Figure 5 shows the experimental layout and the calculation geometry in HIMAC. The target was a stack of 16×16 cm iron plates. Its thickness, 6.85 cm was larger than the range of the projectiles. The center of the target was an independent stack of cylindrical iron plates with 0.15 cm thickness and 4 cm diameter used to verify the direction and positioning of the beam. The target center was positioned to agree with the beam axis with an accuracy of a few millimeters.

A 90-cm-thick ordinary concrete shield was assembled from rectangular blocks measuring $60 \times 15 \times 15$ cm and having a density of 2.27 g/cm^3 . The concrete shield, whose upstream surface had a roughness of less than 1 cm owing to the minor tilts of concrete blocks accumulated from the ground to the top, was located 50 cm downstream from the target.

TABLE 1 Chemical composition of the shielding concrete used for the shielding experiment (Ogawa et al., 2011). The unit is g/cm³.

Hydrogen	Oxygen	Sodium	Magnesium	Aluminum	Silicon	Potassium	Calcium	Iron
0.0237	1.08	0.049	0.02	0.138	0.641	0.0435	0.188	0.0438

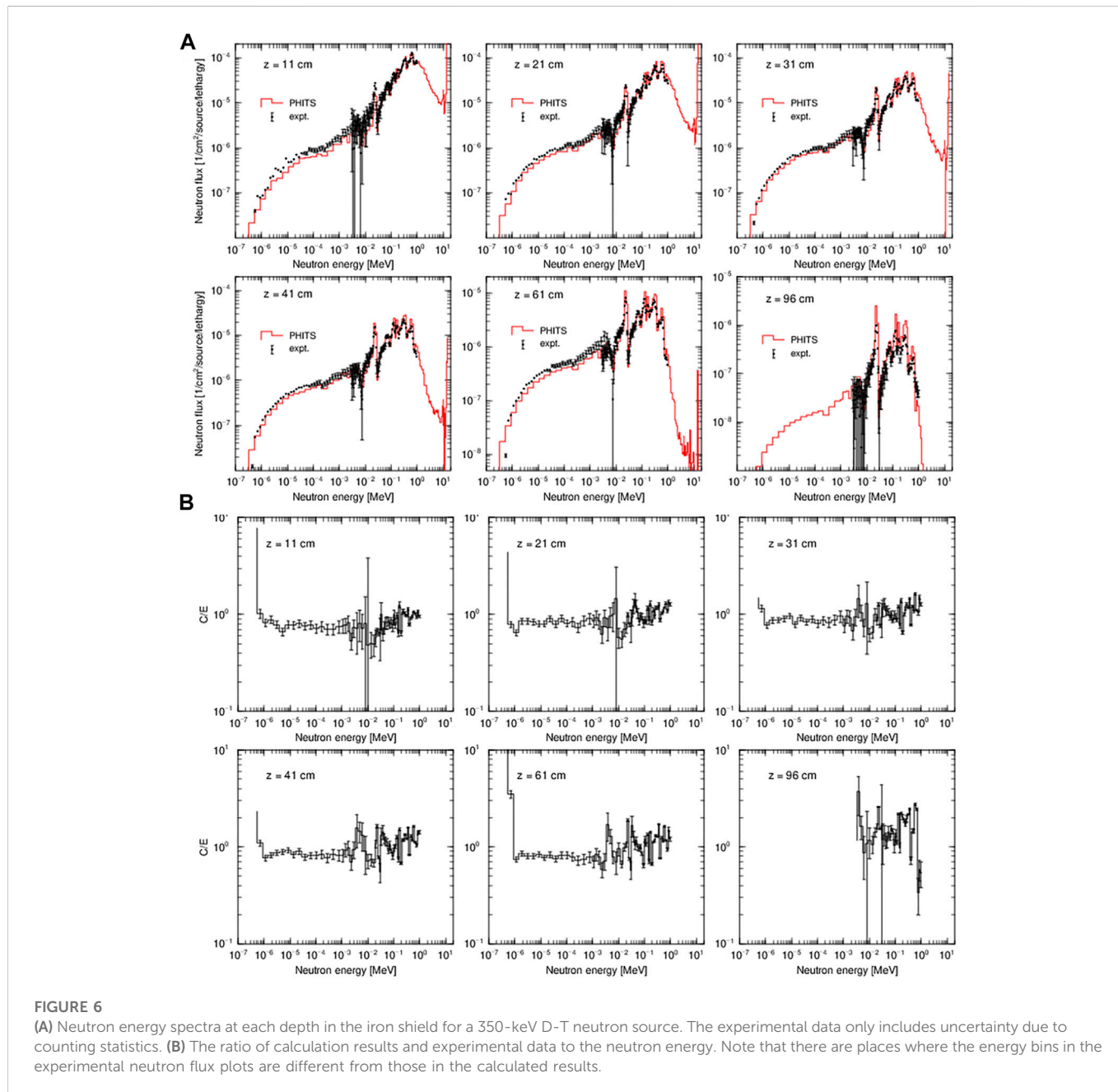


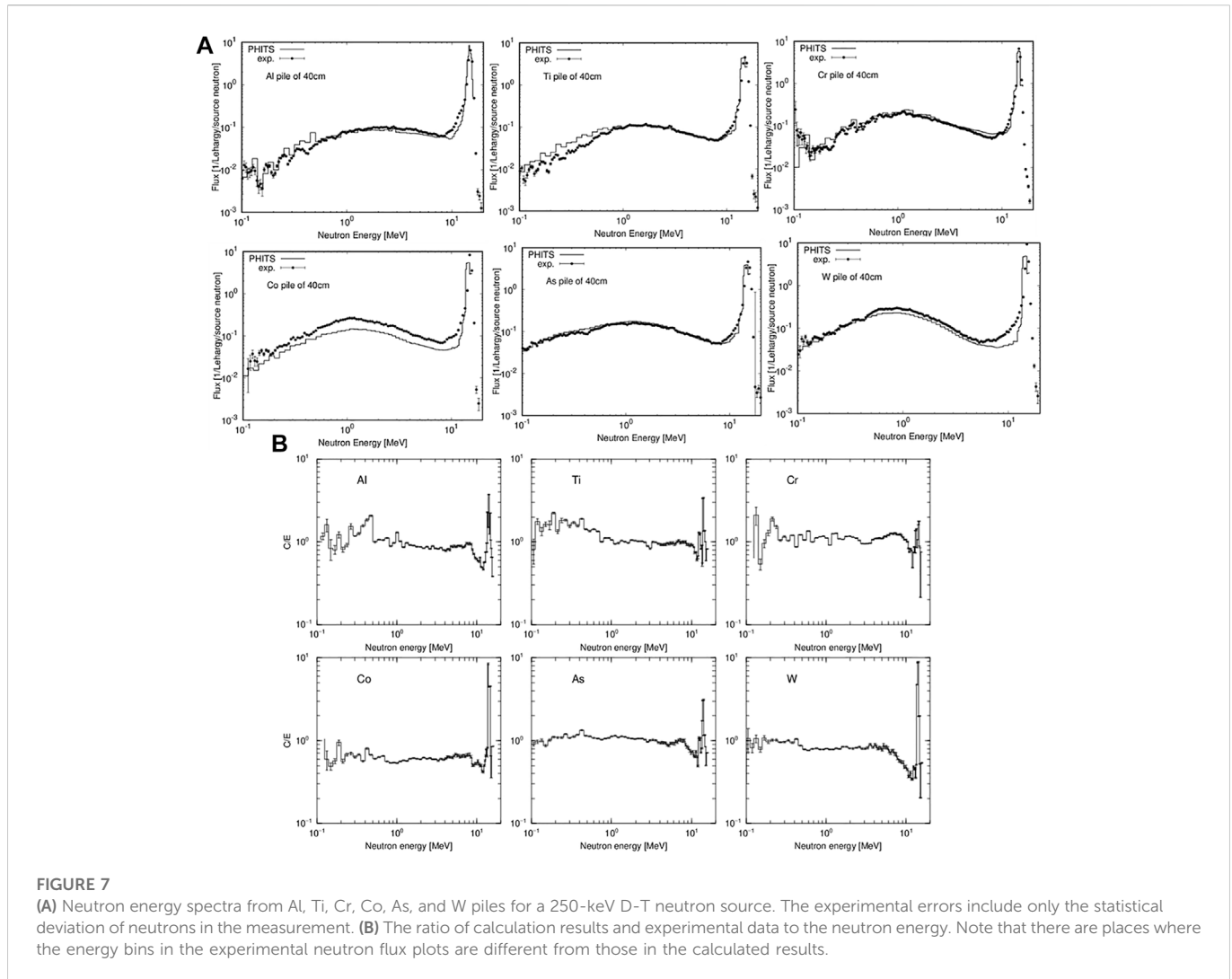
Table 1 shows the chemical composition of the concrete blocks analyzed by using atomic emission spectrometry, atomic absorption spectrometry, and gravimetry. Moisture varies by aging and equilibration in environment but it is fair to assume that the moisture reached equilibrium because the blocks had been stored in the PH1 irradiation room, where the temperature and moisture were kept stable for the accelerator components, for more than 10 years. Owing to the difficulty in chemical composition analysis, carbon was not measured

which is likely to be responsible for the discrepancy between the total density of 2.27 g/cm³ obtained by weighing actual concrete blocks and the sum of the partial densities (Ogawa et al., 2011) of Table 1.

The detectors for activation were set along four parallel lines, at 0, 15, 30, and 45 cm, in the vertical plane that included the beam axis and were shifted below the beam axis. At several depths, thin foils of gold (15 μm thickness), gold (15 μm thickness) covered with cadmium (500 μm thickness) on both sides, and aluminum (1–3 mm thickness)

TABLE 2 C/E with one standard deviation for the accumulated neutron yields in the neutron energy region from 0.003 MeV–10 MeV in the iron shield for a 350-keV D-T neutron source. The experimental data only includes uncertainty due to counting statistics.

Depth (cm)	11	21	31	41	61	96
C/E	1.39 ± 0.01	1.31 ± 0.01	1.24 ± 0.01	1.21 ± 0.01	1.15 ± 0.01	1.78 ± 0.02



activation detectors were placed to measure the activation depth profiles. The ion beams were extracted through an Al beam window with 100 μm thickness as pulses of 400–600-msec-long with 3.3 s repetition intervals. The beam was injected into the target surface and collimated to less than 1 cm in diameter. The iron plate stack, which constituted the central part of the target, was disassembled after irradiation and put on a BAS-MS Imaging Plate to confirm the beam collimation and positioning.

3 Results and discussion

All results are discussed in this section. Numerical data including computational and experimental uncertainties in the figures are

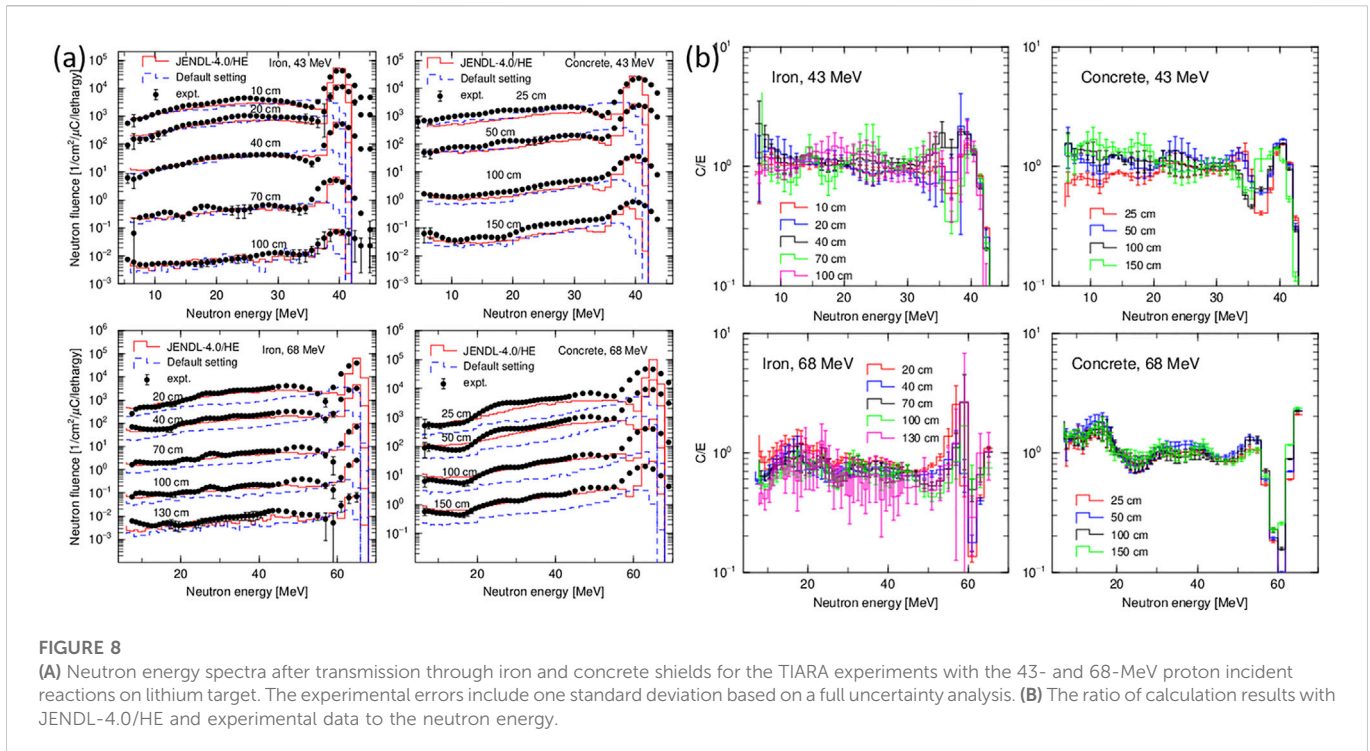
provided as [Supplementary Material](#). In the case of (1), (2), and (3), the ratios of calculated and experimental data and their uncertainties in figures are also included as [Supplementary Material](#).

3.1 Integral experiment on iron cylindrical assembly at FNS

Figure 6A shows neutron energy spectra at 11, 21, 31, 41, 61, and 96 cm from the surface of the iron assembly (Konno et al., 1991; Sub Working Group of Fusion Reactor Physics Subcommittee, 1994). Figure 6B shows the ratio of calculation results and experimental data to the neutron energy. The experimental data only includes uncertainty due to counting statistics. At energies above 50 keV, the

TABLE 3 C/E with one standard deviation for the accumulated neutron yields in the neutron energy region from 0.1 MeV to 15 MeV from Al, Ti, Cr, Co, As, and W piles for a 250-keV D-T neutron source. The experimental data only includes uncertainty due to counting statistics.

Target	Al	Ti	Cr	Co	As	W
C/E	1.028 ± 0.001	1.118 ± 0.002	1.039 ± 0.001	0.804 ± 0.002	1.064 ± 0.002	0.866 ± 0.002



total error of experiments was almost 10% or less. In these spectra, fine structures due to iron resonance were clearly observed around 10, 30, 100, 150, 200, 400, and 800 keV. Table 2 indicates C/E with one standard deviation for the accumulated neutron yields in the neutron energy region from 0.003 MeV–10 MeV in the iron shield for a 350-keV D-T neutron source. Overall, the PHITS calculation results agreed with the experimental data within a factor of 2 as shown in Table 2.

3.2 Leakage neutron spectra from various sphere piles with D-T neutrons

Figure 7A shows the leakage neutron energy spectra from sphere piles of aluminum, titanium, chromium, cobalt, arsenic, and tungsten with D-T neutrons. The experimental errors include only the statistical deviation of neutrons in the measurement. Figure 7B shows the ratio of calculation results and experimental data to the neutron energy. The relative error in measuring the niobium activation foils was less than 1%. The calculated results for Al, Ti, Cr, and As piles reproduce the experimental data within a factor of 1.5 over a wide neutron energy region for all energy bins. The calculated results for a W pile were lower than the experimental data by a factor of 2 at around 10 MeV due to the underestimation of peak neutrons by a factor of 2. The calculated results for a Co pile were lower than the experimental data by a factor of 1–2 below 10 MeV and by a factor of 1.5 at around

15 MeV. Table 3 lists C/E with one standard deviation for the accumulated neutron yields in the neutron energy region from 0.1 MeV–20 MeV from Al, Ti, Cr, Co, As, and W piles for a 250-keV D-T neutron source. The PHITS calculation results agreed with the experimental data within 20%.

3.3 Neutron energy spectra after transmission through concrete and iron shields using a quasi-monoenergetic neutron source

Figure 8A shows the neutron energy spectra after transmission through the iron and concrete shields for the TIARA experiment with the 43- and 68-MeV proton incident reactions on lithium target (NEA, 2022a). The experimental errors include one standard deviation based on a full uncertainty analysis. The solid line shows the results calculated with the proton and neutron data libraries, JENDL-4.0/HE, and the dashed line shows the results with the physics model, INCL4.6 (Boudard et al., 2013). These figures show that the JENDL-4.0/HE can simulate the peak neutron production. The peak indicates the discrete levels of excited nuclei generated by the proton-lithium reaction. JENDL-4.0/HE also reproduces the experimental data well in the continuum part of the energy spectrum. This is because the neutron data for nuclides in the shielding composition of JENDL-4.0/HE was correctly evaluated. Figure 8B shows the ratio of

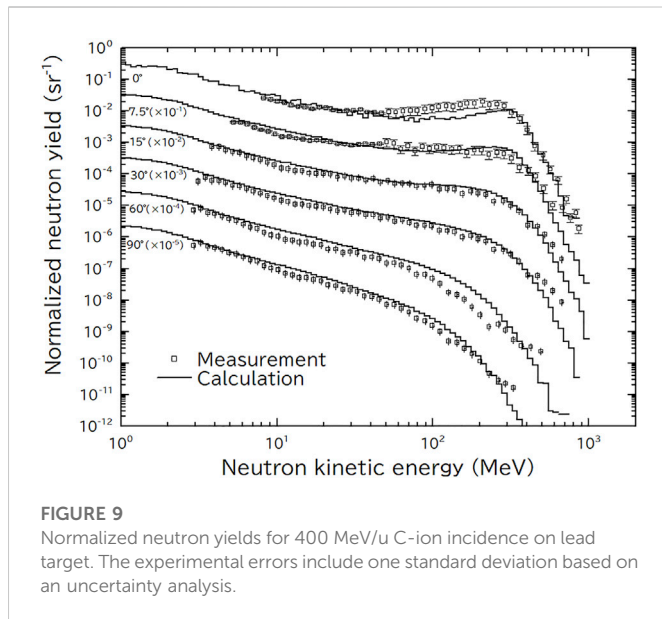


FIGURE 9
Normalized neutron yields for 400 MeV/u C-ion incidence on lead target. The experimental errors include one standard deviation based on an uncertainty analysis.

calculation results with JENDL-4.0/HE and experimental data to the neutron energy. For the 43-MeV proton incidence, the PHITS results agree with the experimental data within a factor of 2 except for the neutron energies below 10 MeV for iron. For the 68-MeV proton incidence, the PHITS results agree with the experimental data within a factor of 2 except for neutron energies around peak.

3.4 Thick target neutron yield produced by heavy-ion incident reaction at HIMAC

Figure 9 presents the measured normalized neutron yields for the lead target irradiated by 400 MeV/u C ions. The neutron detection efficiency of a BC501A was calculated by SCINFUL-QMD code (Sato et al., 2006). The data were measured at various angles and then compared with the results of the calculation by PHITS. A broad peak was found in the yields in the forward direction, 0°. This peak was at the neutron energy equal to about 2/3 of the incident particle energy per ion. It would happen through the peripheral collisions between projectile and target nuclei. An ion strikes directly a neutron of the target nucleus, and transfers its momentum to the neutron. The broad peak energy was moved to a lower energy side and become broad due to the decrease of the incident particle energy in the target material.

Table 4 presents the comparisons between calculation and measurement in terms of accumulated neutron yield, based on a full uncertainty analysis (NEA, 2022b). Though the values of C/E depend on angles, they were found to be within a factor of 2. The evaluation report of these series of measurements using various targets and ion beams in HIMAC will be published in the International Criticality Safety Benchmark Evaluation Project Handbook (NEA, 2022b) by OECD/NEA.

Figure 10 shows the reaction rate distributions of $^{27}\text{Al}(x, \alpha)^{24}\text{Na}$, cadmium-covered $^{197}\text{Au}(n, \gamma)^{198}\text{Au}$ and bare $^{197}\text{Au}(n, \gamma)^{198}\text{Au}$ reactions. The experimental errors include one standard deviation based on an uncertainty analysis. As explained in the figure, the reaction rates along the 4 lines were scaled by 1, 10, 100 and 1,000.

Comparison of the measured and calculated reaction rates shows that the deviation is largest for $^{27}\text{Al}(x, X)^{24}\text{Na}$ reactions along the 15–45 cm axes in the 230 MeV/u He irradiation. This deviation probably came from the overestimation of source term neutrons because spallation induced by helium ions tends to be inaccurate owing to its cluster characteristics. A discrepancy of similar magnitude was observed for cadmium-covered $^{197}\text{Au}(n, \gamma)$ reactions at the depth from 0–20 cm for the 230 MeV/u He beam. Except for the systematic overestimation of $^{27}\text{Al}(x, X)^{24}\text{Na}$ reaction with 230 MeV/u He, the calculated and measured reaction rates at the depth of 60 cm agree within a factor of 2 as shown in Table 5. The reaction rates in the first 20 cm of depth are strongly dependent on the depth therefore a slight fluctuation of the depth leads to a large uncertainty of the ratios. To avoid this uncertainty, the ratios are calculated at 60 cm of depth where the reaction rate decline is exponential.

According to (Ogawa et al., 2011), the thick target neutron yield calculated by PHITS at the forward direction of 230 MeV/u He incident reaction is relatively high with neutron energies below 20 MeV and low with neutron energy above 20 MeV compared with FLUKA code (Ferrari et al., 2005; Battistoni et al., 2007). Moreover, in the first 20 cm of concrete, cadmium-covered $^{197}\text{Au}(n, \gamma)$ reactions are attributed to the source neutrons with energies below 20 MeV down-scattered in the concrete, while the reaction beyond a greater depth is attributed to the neutrons of higher energies. This explains why cadmium-covered $^{197}\text{Au}(n, \gamma)$ reaction rates are overestimated in the first 20 cm while the agreement is good in the deeper region (Ogawa et al., 2011). It means that source neutrons in a few MeV are important as the main contributor of the induced radioactivity maximum, which is found at 10–20 cm of depth.

4 Summary

In this study, we conducted benchmark studies of neutron shielding experiments for fusion, such as (1) Neutron spectra in iron shields with 14 MeV neutrons and (2) Leakage neutron spectra from various piles with D-T neutrons and for Accelerator-Driven Sub-Critical systems, such as (3) Neutron energy spectra after transmission through concrete and iron shields using a quasi-monochromatic neutron source (4) Thick target neutron yield produced by high-energy heavy ion incident reaction in a thick target and (5) Induced activity in shield exposed to particles produced by heavy ion irradiation in a target using the PHITS code.

The calculated neutron energy spectra in the case (1) using the nuclear data libraries, JENDL-4.0, agreed with the experimental data well in iron shields at various depths. For the Al, Ti, Cr, and As piles in the case (2), neutron energy spectra calculated using JENDL-4.0 agreed with the

TABLE 4 C/E with one standard deviation based on a full uncertainty analysis for the accumulated neutron yields for 400 MeV/u C-ion bombardment of lead target.

Angle	0°	7.5°	15°	30°	60°	90°
C/E	0.68 ± 0.16	1.16 ± 0.28	1.27 ± 0.30	1.36 ± 0.33	1.55 ± 0.37	1.35 ± 0.32

Induced activity in shield exposed to secondary particles produced by heavy ions on Fe.

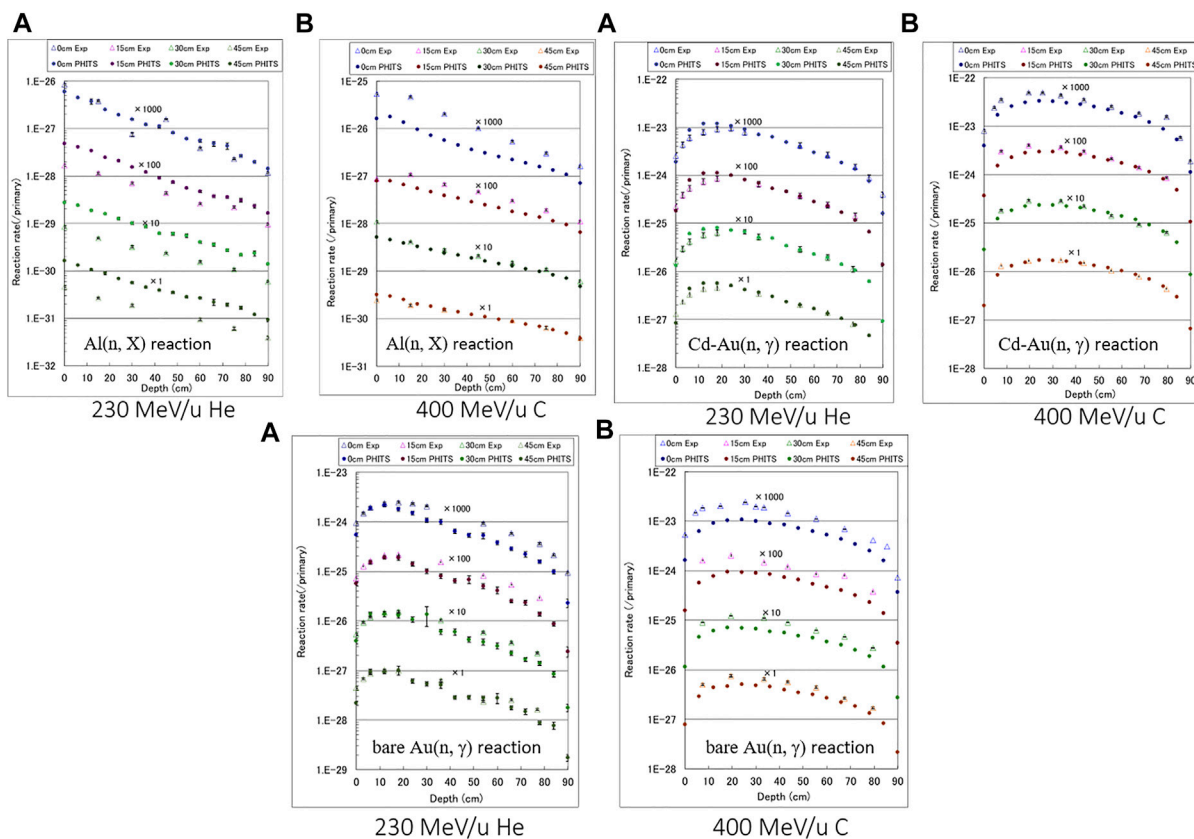


FIGURE 10 Reaction rate distributions of $^{27}\text{Al}(n, X)^{24}\text{Na}$, $^{197}\text{Au}(n, \gamma)^{198}\text{Au}$, and $^{197}\text{Au}(n, \gamma)^{198}\text{Au}$ reactions for (A) 230 MeV/u He reaction and (B) 400 MeV/u C reaction (Ogawa et al., 2011). The experimental errors include one standard deviation based on an uncertainty analysis.

TABLE 5 C/E with one standard deviation for Al(n, X), Cd-Au(n, γ), and bare Au(n, γ) reaction rates at 60 cm of depth. The experimental errors include one standard deviation based on an uncertainty analysis.

Al(n, X) reaction	Lateral coordinate			
	0 cm	15 cm	30 cm	45 cm
(a) 230 MeV/u He	2.30 ± 0.11	2.75 ± 0.14	2.83 ± 0.17	2.47 ± 0.13
(b) 400 MeV/u C	0.41 ± 0.02	0.59 ± 0.03	0.85 ± 0.04	0.95 ± 0.05
Cd-Au(n, γ)	Lateral coordinate			
	0 cm	15 cm	30 cm	45 cm
(a) 230 MeV/u He	0.71 ± 0.05	0.68 ± 0.05	0.68 ± 0.06	0.81 ± 0.05
(b) 400 MeV/u C	0.57 ± 0.03	0.56 ± 0.03	0.67 ± 0.03	0.74 ± 0.03
bare Au(n, γ)	Lateral coordinate			
	0 cm	15 cm	30 cm	45 cm
(a) 230 MeV/u He	1.22 ± 0.13	1.16 ± 0.13	1.03 ± 0.11	0.99 ± 0.11
(b) 400 MeV/u C	0.83 ± 0.03	0.94 ± 0.04	1.15 ± 0.04	1.11 ± 0.04

experimental values well. However, the calculated results for case (2) underestimate the experimental data for Co and W piles. The neutron energy spectra for case (3) using JENDL-4.0/HE reproduced the experimental data well because proton data library for lithium could

simulated this reaction. The proton data library in JENDL-4.0/HE was essential for good reproduction of proton incident reactions. In case (4), the calculated results for a thick target neutron yield produced by 400 MeV per nucleon carbon incident reaction on lead showed good

agreements with the experimental data. For the case (5) with a neutron source produced by the 200–400 MeV per nucleon heavy-ion incident reaction, the calculated results of the reaction rate depth profiles of ^{197}Au (n, γ) ^{198}Au reactions agreed with the experimental data within a factor of 2. Thus, the results of the PHITS calculations using the nuclear data library are in good agreement with the experimental data. Based on these findings, PHITS has been validated for usage in the domain in the design of advanced reactor systems such as fusion and ADS facilities. These experimental data are also useful in validating other Monte Carlo codes and evaluating nuclear data libraries for advanced reactor systems. The usage of the SINBAD database for fusion and ADS applications is also useful in benchmark shielding calculations with all Monte Carlo codes and evaluated nuclear data libraries.

Author contributions

YI, ST conceived the idea of the study. YI, ST, and TO contributed the review of shielding calculations. YI drafted the original manuscript. ST supervised the conduct of this study. YI, ST, and TO reviewed the manuscript draft and revised it critically on intellectual content. YI, ST, and TO approved the final version of the manuscript to be published.

References

- Battistoni, G., Muraro, S., Sala, P. R., Cerutti, F., Ferrari, A., Roesler, S., et al. (2007). "The FLUKA code: Description and benchmarking," in *Proceedings of the hadronic shower simulation workshop 2006, batavia, ILL, 6–8, september 2006*. Editors M. Albrow and R. Raja (Maryland: AIP), 31–49.
- Boudard, A., Cugnon, J., David, J., Leray, S., and Mancusi, D. (2013). New potentialities of the Liege intranuclear cascade model for reactions induced by nucleons and light charged particles. *Phys. Rev. C* 87, 014606. doi:10.1103/PhysRevC.87.014606
- Ferrari, A., Sala, P. R., Fasso, A., and Ranft, J. (2005). *Fluka: A multi-particle transport code*. Washington, D.C: United States. Department of Energy. CERN 2005-10, INFN TC 05/11, SLAC-R-773.
- Furihata, S. (2000). Statistical analysis of light fragment production from medium energy proton-induced reactions. *Nucl. Instrum. Methods Phys. Res. B* 171 (3), 251–258. doi:10.1016/S0168-583X(00)00332-3
- Goorley, T., James, M., Booth, T., Brown, F., Bull, J., Cox, L. J., et al. (2012). Initial MCNP6 release overview. *Nucl. Technol.* 180, 298–315. doi:10.13182/nt11-135
- Iwamoto, Y., Hashimoto, S., Sato, T., Matsuda, N., Kunieda, S., Celik, Y., et al. (2022). Benchmark study of particle and heavy-ion transport code system using shielding integral benchmark archive and database for accelerator-shielding experiments. *J. Nucl. Sci. Technol.* 59, 665–675. doi:10.1080/00223131.2021.1993372
- Iwamoto, Y., Sato, T., Hashimoto, S., Ogawa, T., Furuta, T., Abe, S., et al. (2017). Benchmark study of the recent version of the PHITS code. *J. Nucl. Sci. Technol.* 54, 617–635. doi:10.1080/00223131.2017.1297742
- Kodali, I., Sartori, E., and Kirk, B. (2006). "Sinbad - shielding Benchmark Experiments - status and planned activities," in *Proceedings of the ANS 14th Biennial Topical Meeting of Radiation Protection and Shielding Division, Carlsbad, New Mexico, 2006 April 3–6*.
- Konno, C., Ikeda, Y., Kosako, Y., Oyama, Y., Maekawa, H., Nakamura, T., et al. (1991). Measurement and analysis of low energy neutron spectrum in a large cylindrical iron assembly bombarded by D-T neutrons. *Fusion Eng. Des.* 18, 297–303. doi:10.1016/0920-3796(91)90142-d
- Kos, B., and Kodali, I. (2019). *MCNP modelling of the TIARA SINBAD shielding benchmark, INDC(NDS)-0785*. Austria: IAEA.
- Kunieda, S., Osamu, I., Nobuyuki, I., Tsutomu, O., Futoshi, M., Tatsuhiro, S., et al. (2016). "Overview of JENDL-4.0/HE and benchmark calculation," in *JAEA-Conf 2016-004, Ibaraki, Japan, 19–20 Nov 2015*, 41–46.
- Kurosawa, T., Nakao, N., Nakamura, T., Uwamino, Y., Shibata, T., Nakanishi, N., et al. (1999). Measurements of secondary neutrons produced from thick targets bombarded by high-energy helium and carbon ions. *Nucl. Sci. Eng.* 132, 30–57. doi:10.13182/nse98-53
- Mukaiyama, T., Takizuka, T., Mizumoto, M., Ikeda, Y., Ogawa, T., Hasegawa, A., et al. (2001). Review of research and development of accelerator-driven system in Japan for transmutation of long-lived nuclides. *Prog. Nucl. Energy* 38, 107–134. doi:10.1016/S0149-1970(00)00098-6
- Nakao, N., Nakashima, H., Nakamura, T., Tanaka, S. i., Tanaka, S., Shin, K., et al. (1996). Transmission through shields of quasi-monoenergetic neutrons generated by 43- and 68-MeV protons —I: Concrete shielding experiment and calculation for practical application. *Nucl. Sci. Eng.* 124, 228–242. doi:10.13182/nse96-a28574
- Nakashima, H., Nakao, N., Tanaka, S., Nakamura, T., Shin, K., Sakamoto, Y., et al. (1996). Transmission through shields of quasi-monoenergetic neutrons generated by 43- and 68-MeV protons —ii: Iron shielding experiment and analysis for investigating calculational method and cross-section data. *Nucl. Sci. Eng.* 124, 243–257. doi:10.13182/nse96-a28575
- NEA (2022). International criticality safety benchmark evaluation project (ICSBEP) Handbook. Available at: https://www.oecd-nea.org/jcms/pl_20291/international-criticality-safety-benchmark-evaluation-project-icsbep-handbook (Accessed October 14, 2022).
- NEA (2022). SINBAD website. Boulogne-billancourt. France: OECD/NEA. Available at: https://www.oecd-nea.org/jcms/pl_32139/shielding-integral-benchmark-archive-and-database-sinbad (Accessed October 14, 2022).
- Ogawa, T., Morev, M., N., Iimoto, T., and Kosako, T. (2011). Measurements of induced activity in concrete by secondary particles at forward direction produced by intermediate energy heavy ions on an Fe target. *Nucl. Instrum. Methods B* 269, 1929–1939. doi:10.1016/j.nimb.2011.05.031
- Ogawa, T., Sato, T., Hashimoto, S., Satoh, D., Tsuda, S., and Niita, K. (2015). Energy-dependent fragmentation cross sections of relativistic. *Phys. Rev. C* 92, 024614. doi:10.1103/PhysRevC.92.024614
- ORNL (2022). RSICC website. Available at: <https://www.ornl.gov/onramp/rsicc> (Accessed October 14, 2022).
- Sato, T., Iwamoto, Y., Hashimoto, S., Ogawa, T., Furuta, T., Abe, S., et al. (2018). Features of particle and heavy ion transport code system (PHITS) version 3.02. *J. Nucl. Sci. Technol.* 55, 684–690. doi:10.1080/00223131.2017.1419890
- Satoh, D., Kurosawa, T., Sato, T., Endo, A., Takada, M., Iwase, H., et al. (2007). Reevaluation of secondary neutron spectra from thick targets upon heavy-ion bombardment. *Nucl. Instrum. Methods Phys. Res. A* 583, 507–515. doi:10.1016/j.nima.2007.09.023
- Satoh, D., Sato, T., Shigyo, N., and Ishibashi, K. (2006). "SCINFUL-QMD: Monte Carlo Based Computer Code to calculate response function and detection efficiency of a liquid organic scintillator for neutron energies up to 3 GeV,". *JAEA-Data/Code 2006-023*. Available at: <https://www.osti.gov/etdweb/biblio/20890219>.
- Shibata, K., Iwamoto, O., Nakagawa, T., Iwamoto, N., Ichihara, A., Kunieda, S., et al. (2011). JENDL-4.0: A new library for nuclear science and engineering. *J. Nucl. Sci. Technol.* 48, 1–30. doi:10.1080/18811248.2011.9711675
- Sub Working Group of Fusion Reactor Physics Subcommittee (1994). *Collection of experimental data for fusion Neutronics benchmark*. Tōkai, Ibaraki Prefecture: Japan Atomic Energy Research Institute.

Conflict of interest

The authors declare that the research was conducted in the absence of any commercial or financial relationships that could be construed as a potential conflict of interest.

Publisher's note

All claims expressed in this article are solely those of the authors and do not necessarily represent those of their affiliated organizations, or those of the publisher, the editors and the reviewers. Any product that may be evaluated in this article, or claim that may be made by its manufacturer, is not guaranteed or endorsed by the publisher.

Supplementary material

The Supplementary Material for this article can be found online at: <https://www.frontiersin.org/articles/10.3389/fenrg.2023.1085264/full#supplementary-material>